International Journal of Thermophysics, Vol. 17, No. 2, 1996

An Accurate Van der Waals-Type Equation of State for the Lennard–Jones Fluid

M. Mecke,[1] A. Müller,[1] J. Winkelmann,[1] J. Vrabec,[2] J. Fischer,[3,4] R. Span,[2] and W. Wagner[2]

Received July 30, 1995

A new equation of state (EOS) is proposed for the Helmholtz energy F of the Lennard–Jones fluid which represents the thermodynamic properties over a wide range of temperatures and densities. The EOS is written in the form of a generalized van der Waals equation, $F = F_H + F_A$, where F_H is a hard body contribution and F_A an attractive dispersion force contribution. The expression for F_H is closely related to the hybrid Barker–Henderson pertubation theory. The construction of F_A is accomplished with the Setzmann–Wagner optimization procedure on the basis of virial coefficients and critically assessed computer simulation data. A comparison with the EOS of Johnson et al. shows improvement in the description of the vapor–liquid coexistence properties, the pvT data, and in peculiar, of the caloric properties. A comparison with the EOS of Kolafa and Nezbeda which appeared after the bulk of this work was finished shows still an improvement in the standard deviations of the pressure and internal energy by about 30%.

KEY WORDS: coexistence curve; equation of state; Lennard–Jones fluid; thermodynamic properties.

1. INTRODUCTION

The Lennard–Jones (LJ) fluid is the most widely used model of a simple realistic fluid and, hence, several equations of state (EOS) have been published recently [1–5] to describe its thermodynamic behavior. According to

[1] Institüt für Physikalische Chemie, Universität Halle-Wittenberg, Geusaer Str., D-06217 Merseburg, Germany.
[2] Institut für Thermo- und Fluiddynamik, Ruhr-Universität, D-44780 Bochum, Germany.
[3] Institut für Land-, Umwelt- und Energietechnik, Universität für Bodenkultur, Peter-Jordan Strasse 82, A-1190 Wien, Austria.
[4] To whom correspondence should be addressed.

0195-928X/96/0100-0391$09.50/0

different aims of the authors, different types of equations have been used. Johnson et al. [1] wanted to have a very accurate equation and used a modified Benedict–Webb–Rubin equation. Sowers and Sandler [2], on the other hand, wanted to cast their equation into a form inspired by perturbation theory. Our aim is to find an equation for the Helmholtz energy F in the form of a generalized van der Waals equation, $F = F_H + F_A$, where F_H accounts for the hard body interaction and F_A for the attractive dispersion forces. One reason for equations of this form is that they allow a highly accurate description of real fluids with only a few substance-specific parameters [6]. For mixtures, we believe in agreement with Sowers and Sandler [7] that special mixing rules are required for F_H and F_A and, finally, also for the polar contributions to F [8]. To achieve a satisfying mixing rule for F_A one needs a rather accurate equation for this term. Hence, the aim of this paper is to construct an equation of state for the Lennard–Jones fluid in the form $F = F_H + F_A$, which should be at least as accurate as that of Johnson et al. [1].

The equation is based on simulation data and virial coefficients to be discussed in more detail in the next Section. An optimized equation for F_A is found by the method of Setzmann and Wagner [9].

After the bulk of this work was completed, the very recent equation of Kolafa and Nezbeda [10] came to our attention. Hence, we include also comparisons with this equation.

2. FUNCTIONAL FORM OF THE EQUATION

Let us consider a Lennard–Johnson fluid with the parameters ε and σ and denote all quantities in reduced units. In peculiar, we use the reduced temperature $T^* = kT/\varepsilon$, the reduced density $\rho^* = \rho\sigma^3$, the reduced pressure $p = p\sigma^3/\varepsilon$ and the reduced residual internal energy $u^* = U/N\varepsilon$.

We are looking for an expression of the residual Helmholtz energy F as function of the density ρ and the temperature T, $F = F(\rho, T)$, in the form

$$F = F_H + F_A \tag{1}$$

where F_H accounts for the hard-body interaction and F_A for the attractive dispersion forces.

For a system of hard spheres with a packing fraction ξ the residual Helmholtz energy F_H is given according to Carnahan and Starling [11] as

$$F_H/RT = (4\xi - 3\xi^2)/(1-\xi)^2 \tag{2}$$

For a Lennard–Jones fluid at a given temperature and density, the packing fraction is a quantity with slight arbitrariness. However, Saager et al. [12]

studied its temperature and density dependence using perturbation theories [13–15]. They arrived at the conclusion to describe the temperature dependence of the packing fraction ξ according to the hybrid Barker–Henderson [13] theory and yield the dependence on the density ρ and the temperature T by the correlation

$$\xi = 0.1617(\rho^*/\rho_c^*)[0.689 + 0.311(T^*/T_c^*)^{0.3674}]^{-1} \tag{3}$$

where ρ_c^* and T_c^* are the critical density and temperature, respectively, to be given in the next section.

The crucial point is now the equation for F_A. For that purpose we make an ansatz of the form

$$F_A/RT = \sum_i c_i (T^*/T_c^*)^{m_i} (\rho^*/\rho_c^*)^{n_i} \exp[p_i(\rho^*/\rho_c^*)^{q_i}] \tag{4}$$

where the powers m_i, n_i, p_i, and q_i as well as the coefficients c_i shall be determined by the optimization procedure of Setzmann and Wagner [9].

3. DATA, CRITICAL-POINT CONSTRAINTS AND OPTIMIZATION PROCEDURE

The basic requirement for the construction of an equation of state is a reliable data set. For the gas phase, virial coefficients up to the fifth are available [16], from which we use in this work the second and the third, B and C. With their help thermodynamic properties as pressure, internal energies, and heat capacities can be calculated up to densities $\rho^* \sim 0.1$. On the basis of this truncated virial expansion we have also a criterion to access the accuracy of existing simulation data in the low-density region. At higher densities, we checked the reliability of the simulation data from various sources by the following method. First, we constructed auxiliary equations with all available simulation data which were weighted on the basis of the simulation uncertainties given by the authors. Data points which showed strong deviations from these equations were closer inspected and either reweighted or excluded. At this step careful attention was paid to the simulation methods, the particle numbers and the applied cutoff radius. In the course of the present work we created a new data set which is given in Table I and discussed below.

The data sets which survived this critical data assessment procedure are listed in Table II. From the simulation data in these sets, again, 25% got a lower weighting or were excluded at all in the construction of the EOS.

Table I. Molecular-Dynamics Results from This Work

T^*	ρ^*	p^*	U^*
1.320	0.20	0.12670 (31)	−1.55376(332)
1.320	0.25	0.13135 (45)	−1.89594(304)
1.320	0.30	0.13217 (50)	−2.20336(315)
1.320	0.35	0.13104 (75)	−2.50949(230)
1.320	0.40	0.13367 (98)	−2.80949(244)
1.320	0.45	0.14453 (88)	−3.09978(145)
1.335	0.20	0.13215 (30)	−1.52860(304)
1.335	0.25	0.13728 (35)	−1.88300(318)
1.335	0.30	0.14028 (47)	−2.20077(299)
1.335	0.35	0.14180 (78)	−2.50129(243)
1.335	0.40	0.14333 (83)	−2.78737(167)
1.335	0.45	0.15813(118)	−3.09078(169)

In the construction of any EOS, the critical region and the critical point data are of some interest. In the peculiar form of our EOS, the critical temperature T_c^* and the critical density ρ_c^* are required for the hard-body packing fraction defined in Eq. (3). Recently, a set of parameters was obtained by the $NpT+$test particle method as $T_c^* = 1.314$ and $\rho_c^* = 0.314$ [20]. These data, however, were obtained from correlations for the saturated vapor density ρ'' and the saturated liquid densitiy ρ' forced into the functional form of $\rho' - \rho'' \sim (T_c - T)^{1/3}$. According to experimental evidence, this form holds for nearly infinite ($N \sim 10^{23}$) real systems in the extended critical region. With a decreasing number N of independent particles, however, the critical temperature is believed to increase. Several investigations on that item have been performed recently using the Gibbs ensemble [21–24]. As all the simulation data to which the EOS will be fitted here have been obtained for finite-size systems with up to $N = 1372$ particles, we tried to estimate the critical point of a Lennard–Jones system with about $N \sim 1000$ particles. The above-mentioned studies, however, were not very conclusive for that purpose. Hence, we performed simulations with $N = 1372$ particles at $T^* = 1.320$ and $T^* = 1.335$. The data given in Table I were obtained from molecular-dynamics simulations in a NVT ensemble, i.e., at prescribed particle number N, volume V, and temperature T, with 1372 particles using the momentum scaling method. The equations of motion were solved by a fifth-order predictor–corrector algorithm. Each production run went over 100,000 time steps with the length of a time step of 0.003 in the usual units. The cutoff radius was taken to be half of the box length. The estimation of the statistical uncertainties was made on the basis

Table II. Data Sets Used in the Construction of the Equation of State[a]

Source	Data
Johnson et al. [1]	p^*, u^*
Nicolas et al. [3]	p^*, u^*
Miyano [5]	p^*, u^*
Saager et al. [17]	p^*, u^*
Kolafa et al. [18]	p^*, u^*
Kriebel [19]	p^*, u^*
This work[b]	p^*, u^*
Lotfi et al. [20]	p^*, u^*, p_σ^*, p'^*, p''^*, Δh_v^*
Barker et al. [16]	B^*, C^*

[a] From the simulation data in these sets, again 25% got a lower weighting or were excluded at all in the construction of the equation of state.
[b] See Table I.

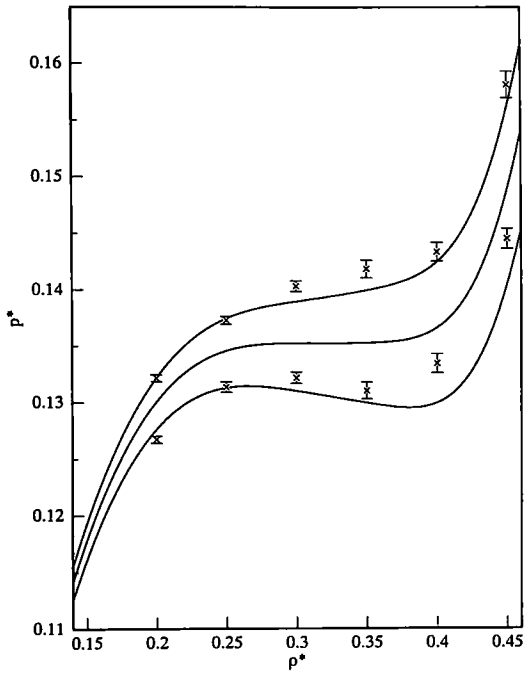

Fig. 1. Pressures from the simulations (Table I) on the isotherms $T^* = 1.320$ and $T^* = 1.335$ together with the values from the new EOS for the same two temperatures and the critical temperature $T^* = 1.328$.

of block averages [25]. From the results in Table I and the graphical representation in Fig. 1, we learn that for that system size the critical point should be somewhere between these two temperatures. This finding is in agreement with a preliminary result of Valleau [26], who estimated $T_c^* = 1.328 \pm 0.003$ for $N = 500$. In view of the fact that it seems difficult to arrive at a more accurate value and in view of the fact that the simulation data to be used in the EOS have been obtained from different particle numbers N, we assumed the critical temperature to be $T_c^* = 1.328$ for the Lennard–Jones fluid of about $N \sim 1000$ particles. This value of T_c^* may still be subject to minor changes in future investigations. After having fixed T_c^*, the critical density was obtained by linear extrapolation of the diameter $(\rho' + \rho'')/2$ from lower temperatures to T_c^* and resulted to be $\rho_c^* = 0.3107$.

As a result of the above discussion, the EOS was constrained to

$$\left(\frac{\partial p}{\partial \rho}\right)_T \Bigg|_{T_c, \rho_c} = 0 \tag{5}$$

and

$$\left(\frac{\partial^2 p}{\partial \rho^2}\right)_T \Bigg|_{T_c, \rho_c} = 0 \tag{6}$$

with $T_c^* = 1.328$ and $\rho_c^* = 0.3107$.

Having fixed the critical quantities, the residual Helmholz energy F_H of the hard-body contribution is given via Eqs. (2) and (3). It remains now to find the contribution of the attractive dispersion forces in the form of Eq. (4). For that purpose we started from the data compiled in Table II and subtracted the hard-body contributions. We were looking then for an ansatz for F_A which minimizes simultanously the standard deviations of the pressures, the internal energies, the enthalpies of evaporation, the Maxwell data for phase equilibrium [20], and the second and third virial coefficients. While the virial coefficients are in principle exact, a small uncertainty had to be assigned to them for technical reasons due to the optimization procedure.

An optimized ansatz for F_A was found by the strategy of Setzmann and Wagner [9]. In that procedure, a "bank of terms" is created by prescribed sets for the powers m_i, n_i, p_i, and q_i in Eq. (4). From this bank of terms the most effective elements are selected by a special search algorithm which combines a stepwise regression analysis with elements of an evolutionary optimization method. Table III contains the powers and coefficients obtained by this procedure for the attractive contribution to the Helmholz energy F_A in the form of Eq. (4).

Table III. Coefficients c_i and Powers m_i, n_i, p_i, and q_i for the Attractive Part of the Helmholtz Energy F_A/RT in Eq. (4)

c	m	n	p	q
$0.33619760720E-05$	−2.0	9	0	0
$-0.14707220591E+01$	−1.0	1	0	0
$-0.11972121043E+00$	−1.0	2	0	0
$-0.11350363539E-04$	−1.0	9	0	0
$-0.26778688896E-04$	−0.5	8	0	0
$0.12755936511E-05$	−0.5	10	0	0
$0.40088615477E-02$	0.5	1	0	0
$0.52305580273E-05$	0.5	7	0	0
$-0.10214454556E-07$	1.0	10	0	0
$-0.14526799362E-01$	−5.0	1	−1	1
$0.64975356409E-01$	−4.0	1	−1	1
$-0.60304755494E-01$	−2.0	1	−1	1
$-0.14925537332E+00$	−2.0	2	−1	1
$-0.31664355868E-03$	−2.0	8	−1	1
$0.28312781935E-01$	−1.0	1	−1	1
$0.13039603845E-03$	−1.0	10	−1	1
$0.10121435381E-01$	0.0	4	−1	1
$-0.15425936014E-04$	0.0	9	−1	1
$-0.61568007279E-01$	−5.0	2	−1	1
$0.76001994423E-02$	−4.0	5	−1	2
$-0.18906040708E+00$	−3.0	1	−1	2
$0.33141311846E+00$	−2.0	2	−1	2
$-0.25229604842E+00$	−2.0	3	−1	2
$0.13145401812E+00$	−2.0	4	−1	2
$-0.48672350917E-01$	−1.0	2	−1	2
$0.14756043863E-02$	−10.0	3	−1	3
$-0.85996667747E-02$	−6.0	4	−1	3
$0.33880247915E-01$	−4.0	2	−1	3
$0.69427495094E-02$	0.0	2	−1	3
$-0.22271531045E-07$	−24.0	5	−1	4
$-0.22656880018E-03$	−10.0	2	−1	4
$0.24056013779E-02$	−2.0	10	−1	4

4. DISCUSSION OF THE NEW EQUATION

The new van der Waals-type EOS for the LJ fluid is given by Eqs. (1)–(4) with $T_c^* = 1.328$, $\rho_c^* = 0.3107$, and the powers and coefficients of F_A/RT from Table III. It covers the whole fluid region up to the highest densities in the temperature range $0.7 \leqslant T^* \leqslant 10.0$ with high accuracy. For still higher temperatures we have ensured that the EOS follows a physically

correct behavior by using simulation data up to $T^* = 100.0$ in the density region $\rho^* \leqslant 1.0$.

The quality of the equation shall be demonstrated by some comparisons with the underlying simulation data for the pressure, the internal energy, and the phase equilibrium data as well as for the specific heat. In these comparisons we also include the modified Benedict–Webb–Rubin (MBWR) equation of Johnson et al. [1] and the pertubed-virial-expansion-hybrid-Barker–Henderson (PVE/hBH) equation of Kolafa and Nezbeda [10], which we believe to be the best presently published EOS.

In the first step we perform a comparison for the pressures and internal energies with the help of the standard deviations

$$\mathrm{STD}_{pvT} = \left(\frac{1}{n} \sum_{i=1}^{n} \frac{(p_{i,\mathrm{EOS}} - p_{i,\mathrm{SIM}})^2}{\Delta p_{i,\mathrm{SIM}}^2} \right)^{1/2} \tag{7}$$

and

$$\mathrm{STD}_{\mathrm{U}} = \left(\frac{1}{n} \sum_{i=1}^{n} \frac{(U_{i,\mathrm{EOS}} - U_{i,\mathrm{SIM}})^2}{\Delta U_{i,\mathrm{SIM}}^2} \right)^{1/2} \tag{8}$$

where n denotes the number of simulation data points, and $p_{i,\mathrm{EOS}}$ and $U_{i,\mathrm{EOS}}$ are the results from the EOS, while the simulation results are assigned as $p_{i,\mathrm{SIM}}$ and $U_{i,\mathrm{SIM}}$ together with their statistical uncertainties $\Delta p_{i,\mathrm{SIM}}$ and $\Delta U_{i,\mathrm{SIM}}$. The results for the standard deviations of the new EOS are shown in Table IV, which also contains the standard deviations of the Johnson et al. [1] equation and of the Kolafa–Nezbeda [10] equation. The standard deviations are shown for three data sets. "Our data set" includes all simulation data used for the contruction of the present EOS in the range of validity of the Johnson et al. [1] EOS, i.e., up to $T^* = 6.0$. The other two data sets are those of Johnson et al. [1] including all molecular-dynamics and Monte Carlo results and of Kolafa et al. [18], with the uncertainties given in the original sources. As one can see from Table IV the new Lennard–Jones EOS gives the smallest weighted standard deviations for our own data set, for the data set of Johnson et al. [1] as well as for the data set of Kolafa et al. [18]. Independently from the used data set the improvement over the Johnson et al. [1] equation is significant especially in the representation of the internal energies. We also find an improvement over the Kolafa–Nezbeda [10] equation by about 20–50%.

The vapor pressures, the saturated liquid densities, and the saturated vapor densities obtained from the new EOS are tabulated in Tables V–VII. These contain also the phase equilibrium data from the MBWR equation [1], the PVE/hBH equation [10], and direct simulation results [20].

Table IV. Standard Deviations for the Pressure and the Internal Energy as Obtained from the New EOS in Comparison to the MBWR Equation of Johnson et al. [1] and to the PVE/hBH Equation of Kolafa and Nezbeda [10] (the Standard Deviations are Shown for Three Data Sets)

	New EOS	MBWR	PVE/hBH
Our data set			
STD_{pvT}	1.0139	1.9031	1.4965
STD_u	0.9777	8.2722	1.3578
Data set of Johnson et al. [1]			
STD_{pvT}	1.5406	2.4688	1.9058
STD_u	1.8040	7.9818	2.2393
Data set of Kolafa et al. [18]			
STD_{pvT}	2.2032	2.7382	2.8544
STD_u	4.2730	19.0787	5.0627

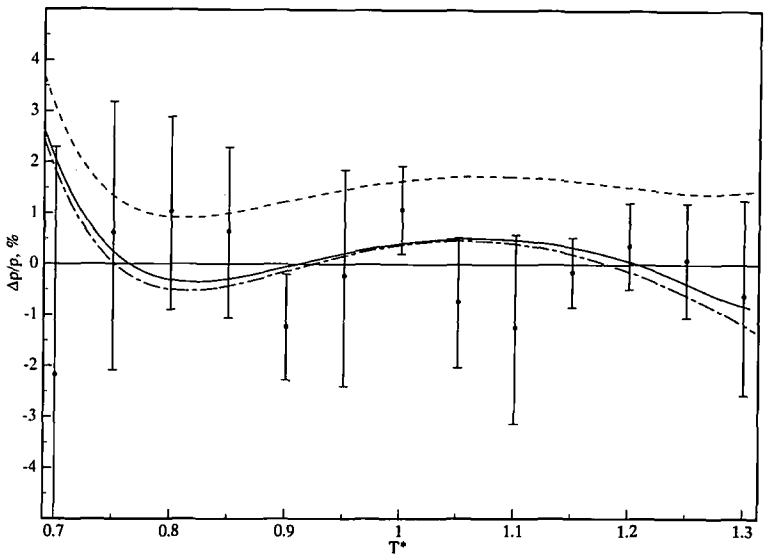

Fig. 2. Deviation plot of the vapor pressures obtained from the new EOS (——), from the MBWR equation of Johnson et al. [1] (– – –), from the PVE/hBH equation of Kolafa and Nezbeda [10] (–·–·–), and direct simulation data [20] (●) in comparison with a correlation, Eq. [20] ($\Delta p/p = (p_\sigma - p_{\sigma,\mathrm{corr}})/p_{\sigma,\mathrm{corr}}$). The error bars indicate the statistical uncertainties of the simulation results.

Table V. Vapor Pressures from the New EOS, from the MBWR Equation of Johnson et al. [1] and from the PVE/hBH Equation of Kolafa and Nezbeda [10] in Comparison with the Simulation Data of Lotfi et al. [20]

	p_σ^*			
T^*	New EOS	MBWR	PVE/hBH	SIM
0.70	0.00137	0.00138	0.00136	0.00131 (6)
0.75	0.00263	0.00266	0.00262	0.00264 (7)
0.80	0.00464	0.00469	0.00463	0.00470 (9)
0.85	0.00762	0.00772	0.00761	0.00769(13)
0.90	0.01182	0.01197	0.01181	0.01168(12)
0.95	0.01749	0.01771	0.01748	0.01741(37)
1.00	0.02488	0.02519	0.02487	0.02505(22)
1.05	0.03426	0.03469	0.03425	0.03384(43)
1.10	0.04589	0.04647	0.04586	0.04511(83)
1.15	0.06003	0.06083	0.05995	0.05974(41)
1.20	0.07694	0.07808	0.07678	0.07718(66)
1.25	0.09684	0.09860	0.09662	0.0973 (11)
1.30	0.12016	0.12290	0.11972	0.1204 (23)

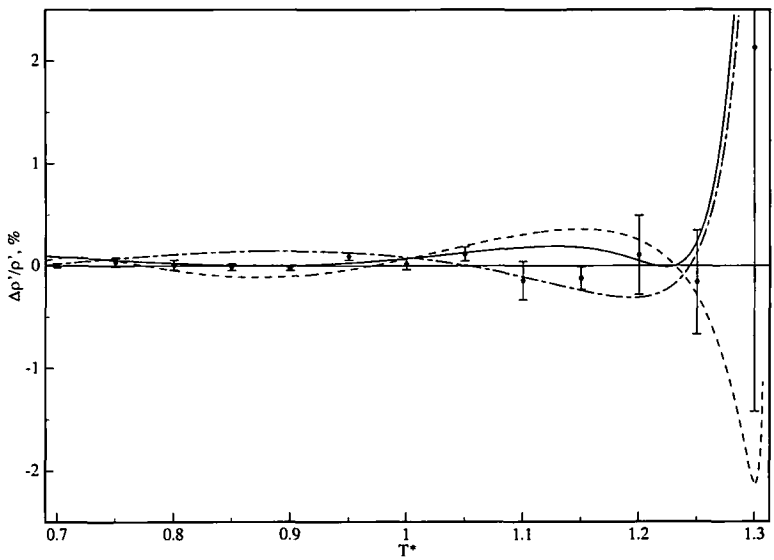

Fig. 3. Deviation plot of the saturated liquid densities obtained from the new EOS (——), from the MBWR equation of Johnson et al. [1] (---), from the PVE/hBH equation of Kolafa and Nezbeda [10] (-·-·-), and direct simulation data [20] (●) in comparison with a correlation, Eq. [20] ($\Delta\rho'/\rho' = (\rho' - \rho'_{\text{corr}})/\rho'_{\text{corr}}$). The error bars indicate the statistical uncertainties of the simulation results.

Table VI. Saturated Liquid Densities from the New EOS, from the MBWR Equation of Johnson et al. [1], and from the PVE/hBH Equation of Kolafa and Nezbeda [10] in Comparison with the Simulation Data of Lotfi et al. [20]

T^*	New EOS	MBWR	PVE/hBH	SIM
0.70	0.84337	0.84324	0.84277	0.84266(18)
0.75	0.82174	0.82169	0.82186	0.82158(38)
0.80	0.79943	0.79887	0.80012	0.79929(39)
0.85	0.77683	0.77551	0.77740	0.77623(25)
0.90	0.75247	0.75166	0.75351	0.75221(13)
0.95	0.72751	0.72703	0.72824	0.72798(27)
1.00	0.70118	0.70117	0.70127	0.70081(38)
1.05	0.67301	0.67345	0.67218	0.67292(46)
1.10	0.64218	0.64300	0.64033	0.6401 (12)
1.15	0.60730	0.60839	0.60475	0.60547(66)
1.20	0.56577	0.56692	0.56375	0.5661 (22)
1.25	0.51452	0.51182	0.51396	0.5125 (26)
1.30	0.45136	0.41020	0.44593	0.428 (15)

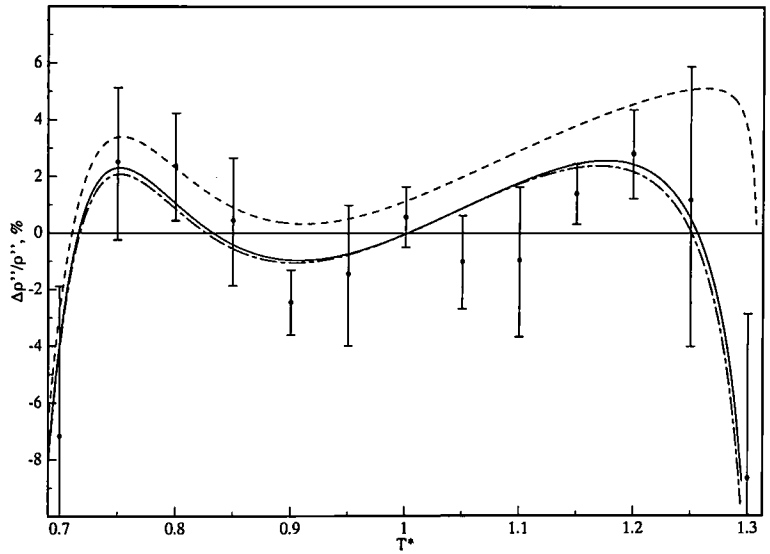

Fig. 4. Deviation plot of the saturated vapor densities obtained from the new EOS (——), from the MBWR equation of Johnson et al. [1] (---), from the PVE/hBH equation of Kolafa and Nezbeda [10] (-·-·-), and direct simulation data [20] (●) in comparison with a correlation, Eq. [20] ($\Delta\rho''/\rho'' = (\rho'' - \rho''_{corr})/\rho''_{corr}$). The error bars indicate the statistical uncertainties of the simulation results.

Deviation plots of these quantities from previous correlation equations [20] are shown in Figs. 2–4. We learn from Figs. 2 and 4 that the vapor pressures and the saturated vapor densities from both, the new EOS and the EOS of Kolafa and Nezbeda [10], are definitely in better agreement with the simulation data than the MBWR results. For the saturated liquid density we learn from Fig. 3 that both new equations offer a slight improvement over MBWR.

Finally, we compare in Table VIII residual isochoric specific heat capacities c_v of the gas from several sources. One source is a truncated virial expansion including the fourth virial coefficient $(B+C+D)$ [16]. In addition, preliminary simulation results from canonical MD simulations using a Nosé–Hoover thermostat are shown, where c_v has been obtained from energy fluctuations [27]. We learn that for the considered state points which are slightly above or just on the dew line, the agreement between these two sources is good. We remind that for the construction of all equations, c_v-values have not been used. We observe that the agreement of the EOS values with those from the truncated virial series and from the simulations becomes worse with increasing density. In this comparison the new EOS behaves slightly better than the PVE/hBH equation.

Table VII. Saturated Vapor Densities from the New EOS, from the MBWR Equation of Johnson et al. [1], and from the PVE/hBH Equation of Kolafa and Nezbeda [10] in Comparison with the Simulation Data of Lotfi et al. [20]

T^*	New EOS	MBWR	PVE/hBH	SIM
0.70	0.00199	0.00201	0.00199	0.00193(10)
0.75	0.00362	0.00366	0.00361	0.00363(10)
0.80	0.00609	0.00616	0.00608	0.00617(12)
0.85	0.00962	0.00974	0.00960	0.00970(22)
0.90	0.01447	0.01466	0.01446	0.01426(16)
0.95	0.02096	0.02122	0.02095	0.02081(51)
1.00	0.02946	0.02981	0.02946	0.02964(32)
1.05	0.04050	0.04096	0.04050	0.03974(65)
1.10	0.05480	0.05543	0.05477	0.0533 (14)
1.15	0.07345	0.07449	0.07335	0.07267(79)
1.20	0.09832	0.10051	0.09805	0.0987 (16)
1.25	0.13300	0.13941	0.13241	0.1339 (67)
1.30	0.18910	0.21978	0.18610	0.195 (11)

Table VIII. Residual Isochoric Heat Capacities of the Gas from a Truncated Virial Expansion ($B+C+D$) [16], from Canonical Molecular-Dynamics Simulations [27], from the New EOS, from the MBWR Equation [1], and from the PVE/hBH Equation [10]

		c_v^*				
T^*	ρ^*	Virial	SIM	New EOS	MBWR	PVE/hBH
1.15	0.0533	0.263	0.243	0.254	0.227	0.247
1.10	0.0533	0.310	0.293	0.293	0.258	0.281
1.25	0.0987	0.416	0.488	0.384	0.343	0.370
1.20	0.0987	0.500	0.544	0.439	0.387	0.417
1.35	0.195	0.685	0.684	0.543	0.511	0.514
1.30	0.195	0.859	0.803	0.617	0.573	0.574

Concluding, we can state that we have constructed an EOS for the Lennard–Jones fluid in the form of a generalized van der Waals equation which is definitely in better agreement with the existing simulation data than the MBWR equation of Johnson et al. [1] and shows still a slight improvement over the PVE/hBH equation of Kolafa and Nezbeda [10].

ACKNOWLEDGMENTS

The authors thank Professor J. P. Valleau and Dozent I. Szalai for communicating results prior to publication. This work was supported by the Deutsche Forschungsgemeinschaft, Az. Wi 1081/1-3 and Fi 287/8-2.

REFERENCES

1. J. K. Johnson, J. A. Zollweg, and K. E. Gubbins, *Mol. Phys.* **78**:591 (1993).
2. G. M. Sowers and S. I. Sandler, *Fluid Phase Equil.* **67**:127 (1991).
3. J. J. Nicolas, K. E. Gubbins, W. B. Street, and D. J. Tildesley, *Mol. Phys.* **37**:1429 (1979).
4. N. K. Koutras, V. I. Harismiadis, and D. P. Tassios, *Fluid Phase Equil.* **77**:13 (1992).
5. Y. Miyano, *Fluid Phase Equil.* **85**:71 (1993).
6. B. Saager and J. Fischer, *Fluid Phase Equil.* **93**:101 (1994).
7. G. M. Sowers and S. I. Sandler, *AIChE J.* **39**:663 (1993).
8. A. Müller, J. Winkelmann, and J. Fischer, *Fluid Phase Equil.* (1996), in press.
9. U. Setzmann and W. Wagner, *Int. J. Thermophys.* **10**:1103 (1989).
10. J. Kolafa and I. Nezbeda, *Fluid Phase Equil.* **100**:1 (1994).
11. N. F. Carnahan and K. E. Starling, *J. Chem. Phys.* **51**:635 (1969).
12. B. Saager, R. Hennenberg, and J. Fischer, *Fluid Phase Equil.* **72**:41 (1992).
13. W. R. Smith, in *Specialist Periodical Reports, Statistical Mechanics, Vol. 1*, K. Singer, ed. (Chem. Soc., Londen, 1973), p. 71.

14. J. A. Barker and D. Henderson, *J. Chem. Phys.* **47**:4714 (1967).
15. J. Fischer, R. Lustig, H. Breitenfelder-Manske, and W. Lemming, *Mol. Phys.* **52**:485 (1984).
16. J. A. Barker, P. J. Leonard, and A. Pompe, *J. Chem. Phys.* **44**:4206 (1966).
17. B. Saager and J. Fischer, *Fluid Phase Equil.* **57**:35 (1990).
18. J. Kolafa, H. L. Vörtler, K. Aim, and I. Nezbeda, *Mol. Sim.* **11**:305 (1993).
19. C. Kriebel, *Dipl.-Chem. thesis* (Institut für Physikalische Chemie, Martin-Luther-Universität Halle-Wittenberg, 1993).
20. A. Lotfi, J. Vrabec, and J. Fischer, *Mol. Phys.* **76**:1319 (1992).
21. K. K. Mon and K. Binder, *J. Chem. Phys.* **96**:6989 (1992).
22. B. Smit, *J. Chem. Phys.* **96**:8639 (1992).
23. A. Z. Panagiotopoulos, *Int. J. Thermophys.* **15**:1057 (1994).
24. L. Vega, E. de Miguel, L. F. Rull, G. Jackson, and I. A. McLure, *J. Chem. Phys.* **96**:2296 (1992).
25. D. Fincham, N. Quirke, and D. J. Tildesley, *J. Chem. Phys.* **84**:4535 (1986).
26. J. P. Valleau, *private communication*, (1994).
27. Szalai, J. Liszi, and J. Fischer, *private communication*, (1994).